

Reconstruction of Centennial Series of Solar Activity

K. A. Tlatova^{a, *}, V. V. Vasil'eva^a, N. N. Skorbezh^a, E. A. Illarionov^b, and A. G. Tlatov^{a, c}

^a*Kislovodsk Mountain Astronomical Station, Central Astronomical Observatory,
Russian Academy of Sciences, Kislovodsk, Russia*

^b*Moscow State University, Russian Academy of Sciences, Moscow, Russia*

^c*Kalmyk State University, Elista, Russia*

**e-mail: k.tlatova@mail.ru*

Received February 15, 2018

Abstract—The results of the digitalization of the centennial series of solar activity are considered. The data contain information on sunspots since 1918, sunspot umbra since 1917, plages since 1907, and spectral corona since 1939. In particular the digitalization of prominences from the observations in the Ca II K line in 1910–1954 and solar filaments from the observations in the H-alpha line in 1912–2002 acquired at the Kodaikanal Observatory are described. The methods of constructing composite maps of solar activity and presenting the resulting data series on the Internet are described. The long-term variations in solar activity are analyzed.

DOI: 10.1134/S0016793218080182

1. INTRODUCTION

Solar-terrestrial connections depend on solar activity, which exhibits short-term and long-term variations. At the present time, it is possible to estimate the level of influence of the solar activity by a comprehensive approach based on a comparison of current observations with the long-term observational data. For these purposes, the pattern of solar activity in the past needs to be recovered as completely as possible.

There are several approaches to solving this problem. One method of extracting the new information from the data of long-term photographic observations is the creation of intensity maps and the subsequent reconstruction of pseudomagnetograms. As a rule, this is performed using the observational data in the Ca II K line (Ortiz and Rast, 2005). The emission in this line is assumed to be conditioned by the existence of regions with an increased concentration of magnetic fields (Pevtsov et al., 2016). Using this fact, it is possible to propose analogs of the magnetic field intensity maps (Bertello et al., 2016). By combining them with maps of the polarity of the large-scale magnetic field (McIntosh, 1974; Makarov and Sivaraman, 1989), it is possible to construct pseudomagnetograms, which will also take into account the sign of the large-scale magnetic field. The complexity of this approach lies in the fact that the intensity depends on multiple factors that are difficult to take into account, such as the process of photoexposure, position of the spectral line relative to the exit slit, and photoemulsion sensitivity. When these parameters affect the intensity in a wide range of values, it is challenging to use the

intensity recorded on a photoplate to determine the magnitude of the magnetic field.

Another approach consists in identifying the structures of activity in archived photographs or sketches of solar activity. In this approach, the outlines of the activity elements, e.g., sunspots, plages, or filaments, are distinguished visually or using computer algorithms. This approach is convenient for verifying the data and creating new activity indices, such as the area of filaments or the number of bright high-latitude elements visible in the Ca II K line. In our study, we reconstruct the data using the second approach. It should be noted that this approach is more laborious, since it requires the manual calibration of the initial observational data and visual identification of structures.

At the present time, the following results regarding the digitalization of long-term series of observations have been achieved.

1. The outlines of sunspots have been distinguished in the daily data of the photographic archives of the Royal Greenwich Observatory (RGO) from 1918–1972 and Kislovodsk Mountain Station from 1954–2017. As a result, a catalog of sunspot groups and individual sunspots listing their various geometric characteristics was compiled. The volume of the digitized RGO plates was approximately 13000 plates, in which more than 242000 individual sunspots in total were identified (Skorbezh et al., 2016). The digitalization of the photoheliograms from the Mountain Station presently continues.

2. The digitalization of the sunspots' magnetic fields from the Mount Wilson Observatory data was performed. In total, approximately 20000 daily

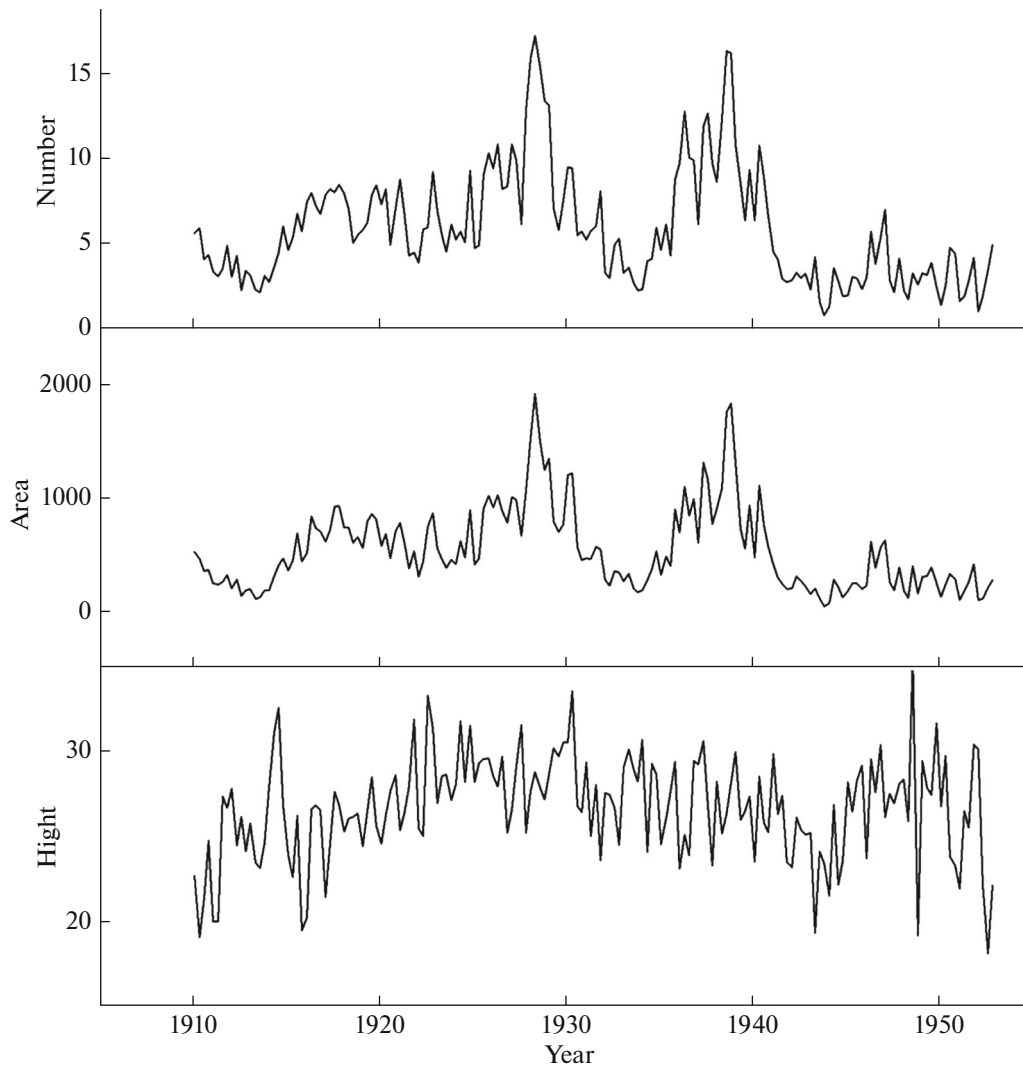


Fig. 1. Results of distinguishing prominences in digitized photoplates of Kodaikanal observatory in Ca II K line averaged over 3 months: (a) number of distinguished prominences per day; (b) average area of prominences in units of $\text{arcsec}^2/10$; (c) average altitude of prominence in arcseconds.

sketches of sunspots, umbra, and pores with measured magnetic fields were processed for 1917–2016. There was a total of digitized 435662 magnetic field measurements for individual umbra and pores (Tlatova et al., 2015).

3. The solar prominences from the visual observation data for 1922–1934 (activity cycle 16) were digitized. In total, more than 51000 prominences for 4708 observation days were identified from these data (Tlatova and Nagnibeda, 2017).

4. More than 90000 prominences from the daily observations in the Ca II K line at the Kodaikanal Observatory were distinguished in 1910–1954 (see Section 3).

5. The solar filaments in the H-alpha line images from the Kodaikanal Observatory were digitalized. In total, more than 326000 filaments in 24308 images of the Kodaikanal observatory were identified in 1912–2002 (see Section 4) (Tlatova et al., 2017).

6. A series of the intensity of the spectral corona in lines Fe XIV 5303 Å and Fe XIV 6374 Å were constructed based on the observational data from coronal observatories for 1939–2017 (Aliev et al., 2017).

7. The boundaries of coronal holes were distinguished based on the data from ground-based and space observatories since 1975 (Tlatova et al., 2014).

The processed and digitized archived observations are complemented with modern observations from the Kislovodsk Mountain Astronomical Station of the Central Astronomical Observatory of the Russian Academy of Sciences, where images have been digitally processed since 2004. It is important to note that both historic and contemporary data were processed using the same method and comprise a detailed picture of solar activity from the beginning of the 20th century to the present time. Further, Sections 3–5 of this paper pres-

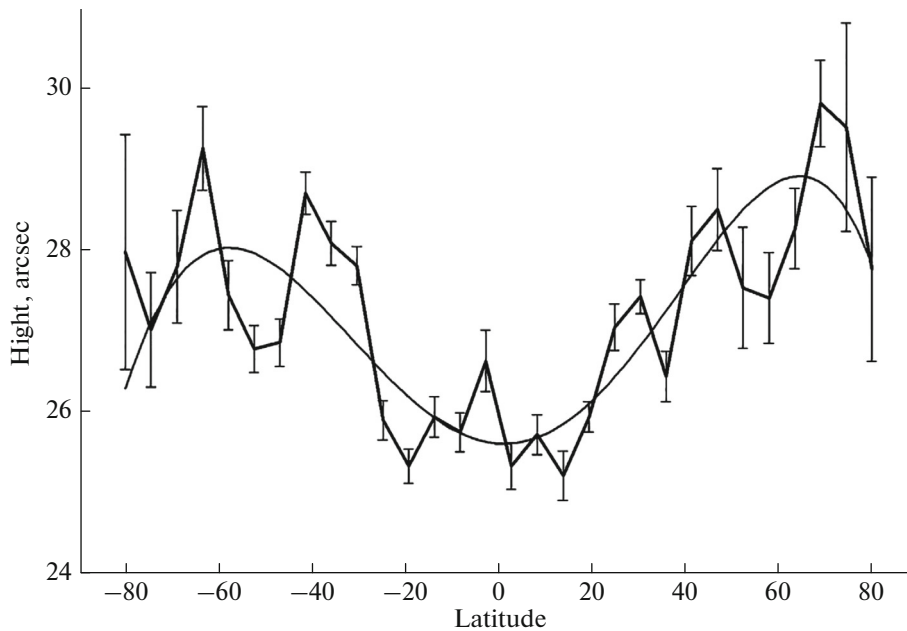


Fig. 2. Latitudinal distribution of average altitude of prominences for 1910–1952. Confidence interval and approximation with fourth-order polynomial are shown (red line).

ent the details of the digitalization of the data and construction of composite activity maps; Section 6 describes the internet website where the activity maps are published.

3. IDENTIFYING THE PROMINENCES FROM OBSERVATIONS IN THE Ca II K LINE

Unlike the present time, there were fewer data sources in the first half of the 20th century that allowed reliable extraction of information on prominences. A potential source of such data is the archive of observations from the global network of visual solar spectroscopes (for 1922–1934). However, as shown in (Tlatova and Nagnibeda, 2017), the large number of observational stations and inconsistency of the methods for forming the sketches leads to the necessity of reverification of the data and hinders an adequate recovery of the actual shapes, areas, and altitudes of prominences.

At the same time, regular observations of the chromosphere in the Ca II K line at the Kodaikanal Observatory (India) provide an opportunity for identifying the prominences on photographic plates. Since the Mountain Station has the experience, methods, and software for identifying the prominences which were acquired within the synoptic program of the Solar Service, we applied these methods to process the archived observations.

The processing procedure consists of several stages. The first stage consists of searching for points belonging to the solar disk, determining the North Pole pole marker, and overlaying the heliographic grid. Further, the background above the solar disc is subtracted in

order to increase the contrast of prominences. After that, the program identifies bright objects above the solar disc.

However, since the initial image of the solar disc on the spectroheliograph often differs from an ideal circle, some of the identified points can in fact belong to the solar disc itself. At the second stage, they are eliminated using the method of refining the local positions of the points of the limb for those segments where a bright object (prominence) was identified at the first stage.

The final stage consists in the manual editing of the identified objects, and in particular, removing the false objects produced by artifacts, such as a flare light on the photoplate, scratches, and clouds.

The result of the identification of the prominences contains the coordinates of the object's boundaries and a set of its parameters: the area of prominences in units of $\text{arcsecond}^2/10$ ($1 \text{ arcsecond}^2/10 \sim 5.26 \times 10^4 \text{ km}^2$) and the altitude of the prominence in arcseconds ($1 \text{ arcsecond} \sim 725.4 \text{ km}$).

A total of more than 90000 prominences was distinguished over 1910–1954. Figure 4 shows the variations in the number of prominences, as well as their average area and altitude. Note that the local peaks of 1928 and 1937 correspond to the maximum activity in cycles 16 and 17. At the same time, these maximums are not seen clearly in cycles 15 and 16, which is probably due to the quality of the images.

Figure 5 shows the distribution of prominences with latitude. It can be noted that the altitude of prominences at middle and high latitudes is higher than in the region of the formation of sunspots. Possibly, this

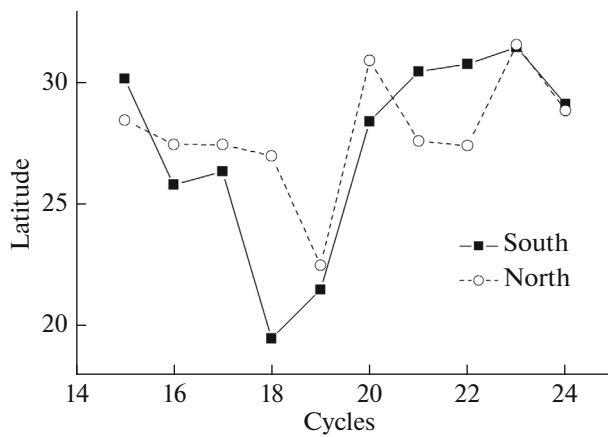


Fig. 3. Variations in average latitudes of prominences based on distribution maximums for northern and southern hemispheres for cycles 15–24.

is due to the presence of two types of prominences: low latitudes are dominated by the prominences of active regions, while high latitudes are dominated by quiet prominences.

In (Tlatova and Nagnibeda, 2017), the distribution of prominences with latitude for cycles 16 and 19–24 was discussed. The digitalization of prominences in the Ca II K line made it possible to add new information on cycles 15–18. Figure 6 shows the variations in the maximums of the latitudinal distributions of prominences for cycles 15–24. In our opinion, the long-term variations may be associated with the centennial cycles of activity.

The prominences are present at all solar latitudes. This allows us to analyze the prominence activity, in particular, at high latitudes. Various data on prominences were used: the digitalization based on the atlases by Wolfer (Vasil'eva, 2006) for 1887–1889 and 1904–1910; the digitalized data on prominences in the Ca II K line for 1910–1954; and the data from the Kis-

lovodsk Mountain Astronomical Station, Central Astronomical Observatory (MAS CAO) for 1957–2017. Further, we constructed the latitude–time diagrams and mapped the positions of the drift of the high-latitude prominences. In the case of a triple polarity reversal, the prominences belonging to the first reversal were taken. Figure 4 shows the trajectories of the median line of the drift of polar prominences in the northern hemisphere for cycles 13–24, scaled to the same interval of time. It turned out that there the drift rate of polar prominences cannot be unambiguously connected with the amplitude of the sunspot cycle. For example, it can be noted that the trajectory of the drift of polar prominences for cycle 19 is located between cycles 20 and 24.

4. CHARACTERISTICS OF SOLAR FILAMENTS

The digitized data of the long-term observational series make it possible to trace the time variations in various solar activity parameters. This section of the paper presents the results of the analysis of long-term variations in the filaments based on the digitized data of the observations in the H-alpha line for 1912–2002. Figure 5 shows the mean monthly values of the area of solar filaments and total length of the filaments in comparison with the sunspot activity. It can be noted that these parameters exhibit a distinct 11-year variation. The length and area of the filaments reached their maximum in activity cycle 19. The relatively small values of these parameters in cycle 18 are possibly due to the low quality of the photoplates in the postwar period.

Figure 5 presents the distribution of filaments in the latitude–time diagram considering the tilt angles of the filaments with respect to the equator. The filaments in the diagram are colored red if their east ends are closer to the poles than their west ends and blue in the opposite case. Note that, on average, the red color prevails in the low-latitude zone, while the blue color

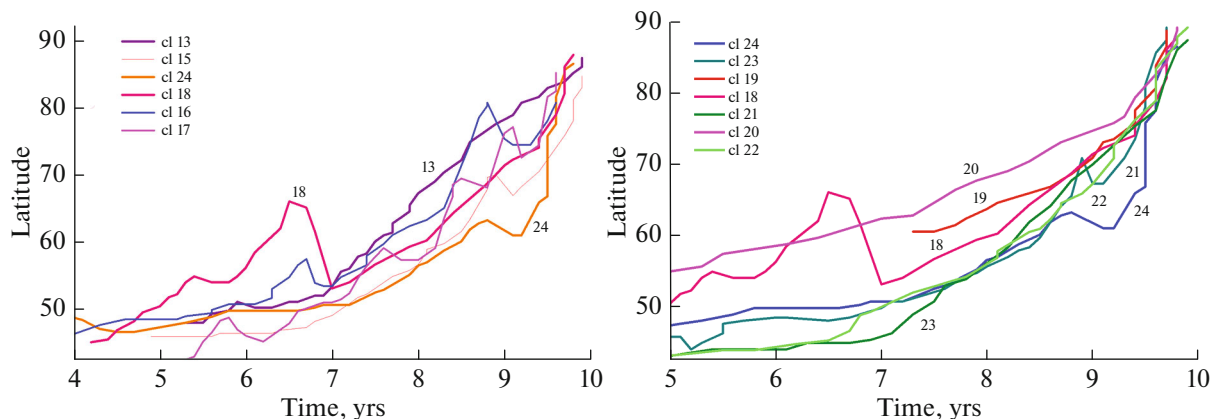


Fig. 4. Drifts of polar prominences in northern hemisphere for cycles 13–18 and 24 (left) and cycles 19–24 (right) scaled to same interval of time.

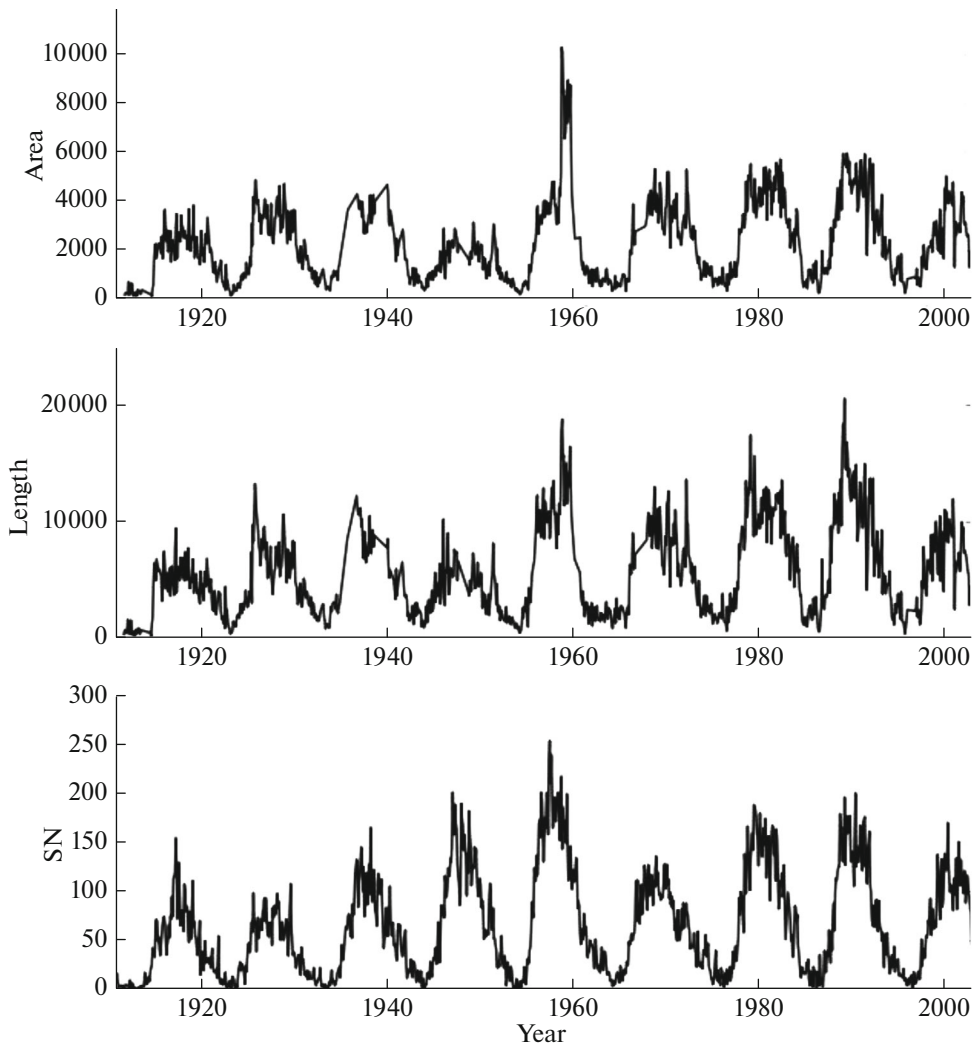


Fig. 5. Mean monthly values of areas of solar filaments measured in mvh (top panel); lengths of filaments in Mm (middle panel); sunspot index (bottom panel).

prevails at high latitudes. This is also confirmed by Diagram 5, which shows the average tilt angles of the filaments as a function of latitude. At latitudes above 40° the filament tilt angles become reversed. Note that similar results were obtained earlier in (Tlatov et al., 2016). However, it is still unclear how this effect can be explained.

5. RECONSTRUCTION OF THE ACTIVITY MAPS

The digitalization of the long-term data series makes it possible to reconstruct the daily maps of solar activity at various altitudes of the solar atmosphere. Figure 7 presents the daily activity map for January 10, 1959. That year was characterized by a high level of solar activity. The maps show the sunspots identified during the digitalization of the photoheliograph observations at the RGO and Kislovodsk (Skorbezh et al., 2016); the plages observed in the Ca II K line from the data of the

observatories of Kodaikanal, Mount Wilson, Sacramento Peak, and Kislovodsk (Tlatov et al., 2009); solar filaments from the observational data of the Kodaikanal Observatory (Tlatova et al., 2017); prominences (Tlatova and Nagnibeda, 2017); solar corona in the 5303 Å and 6374 Å lines (Aliev et al., 2017); and the boundaries of coronal holes (Tlatov et al., 2014).

An important step in mapping the objects on a composite map is the recalculation of the coordinates to the heliographic grid fixed at a chosen time point. As a rule, such a time point is the time when the photographs of sunspots (photoheliograms) were taken. In this case, other kinds of observations are recalculated up to this moment. For the recalculation, we used the assumption on the solid body rotation of the Sun with a period equal to the Carrington rotation, $T_{\text{car}} = 27.2753$ days. The procedure consisted of several steps. First, the difference of the observation times Δt was calculated. Further, each point of the solar activity ele-

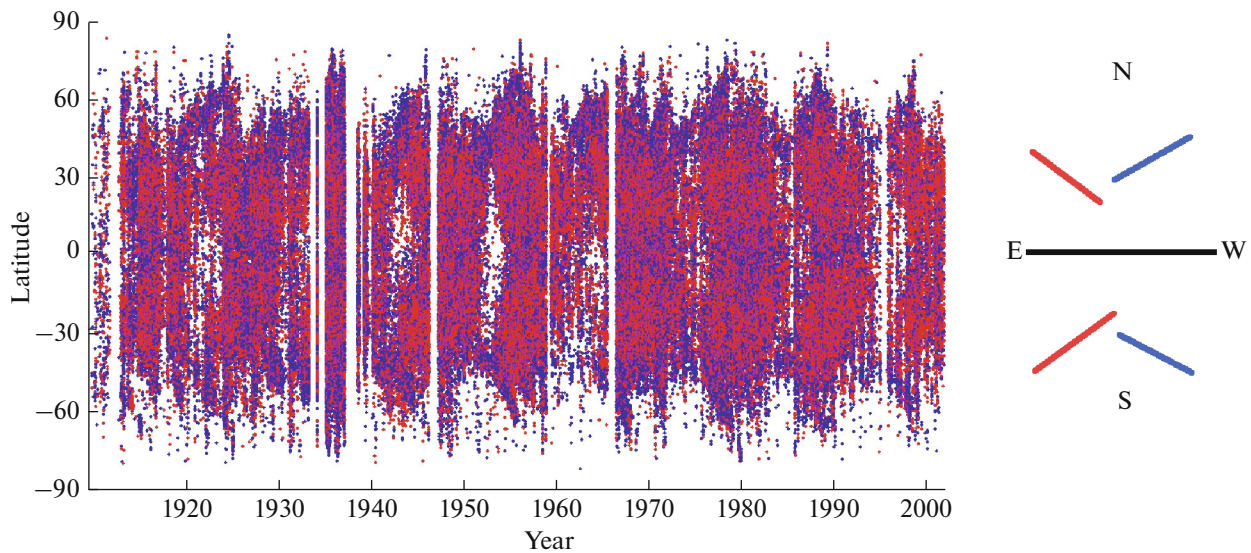


Fig. 6. Distribution of filaments on latitude–time diagram considering tilt angles of filaments with respect to equator. Filaments are marked in red if their eastern ends are closer to poles than their western ends and they are marked in blue in opposite case (see diagram on left).

ments was recalculated to the new heliographic grid with the longitude shift $\Delta\phi = \Delta t T_{\text{car}}$.

Aside from the reconstruction of the daily activity maps, the recovery of synoptic maps of the solar activity is just as important. Such synoptic maps were created, for example, by the Medon Observatory for 1919–2003. There are well-known maps by P. MacIntosh (MacIntosh, 1973) (1964–2009) (<https://www2.hao.ucar.edu/mcintosh-archive/four-cycles-solar-synoptic-maps>),

from the Kislovodsk Mountain Astronomical Station (1978–2016) (<http://solarstation.ru/>), and maps of the polarity division of a large-scale magnetic field (1915–1964) (Makarov and Sivaraman, 1989).

At the same time, these series of synoptic maps have several disadvantages. One disadvantage is the fact that the catalog of maps refers to one observatory only and, as a rule, contains a very limited series of observational days. However, the main disadvantage is the format of the synoptic maps: they are stored as printed material or pixel images. For this reason, editing the maps requires redigitalization (Tlatov et al., 2016).

The new digital synoptic maps are important for the recovery of the solar magnetic field from the observational data in the Ca II K line (Pevtsov et al., 2016). The observations in the Ca II K line can provide information on the magnetic field intensity. However, to determine the polarity of the magnetic fields, it is necessary to include the observations of prominences and filaments. We construct the composite activity maps which can be used for the recovery of the magnetic field over the whole surface of the Sun, as well as for numerous other tasks. Figure 8 shows a composite synoptic map with sunspots, sunspot umbra, plages observed in the Ca II K line, prominences, and filaments.

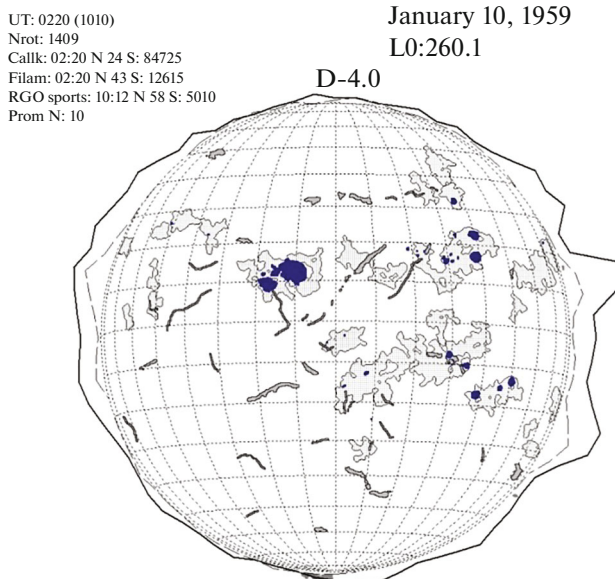


Fig. 7. Composite solar activity map for January 10, 1959. Map shows positions of sunspots (blue color); plages in Ca II K line (regions with dotted shading); filaments (in gray); prominences and solar corona intensities in 5303 Å (solid line) and 6374 Å (dashed line) lines.

6. PUBLICATION OF THE DIGITALIZATION RESULTS ON THE INTERNET

We plan to publish all the digitized data to be openly available on the Internet. The website www.observethesun.com, which combines the data of operative monitoring and archived observations of

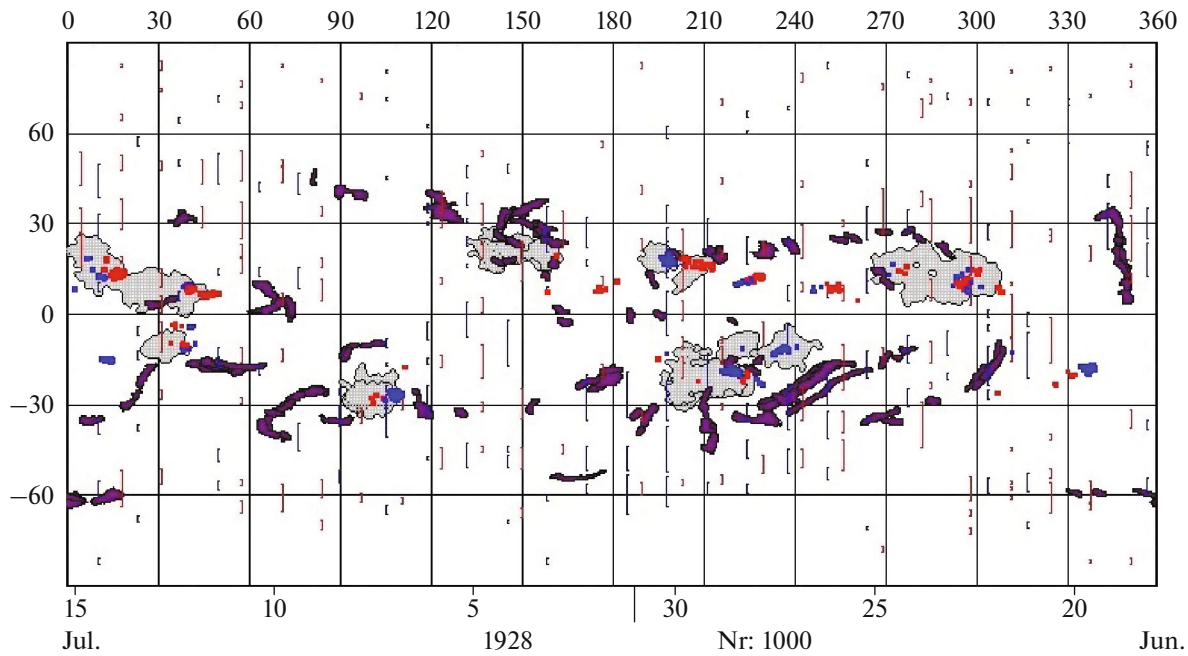


Fig. 8. Composite synoptic map for rotation N1000, June–July, 1928. Map shows sunspot umbra (blue and red areas); plages (gray area) observed in Ca II K line; prominences (vertical parts oriented to right for eastern limb or to left for western limb); and filaments (purple).

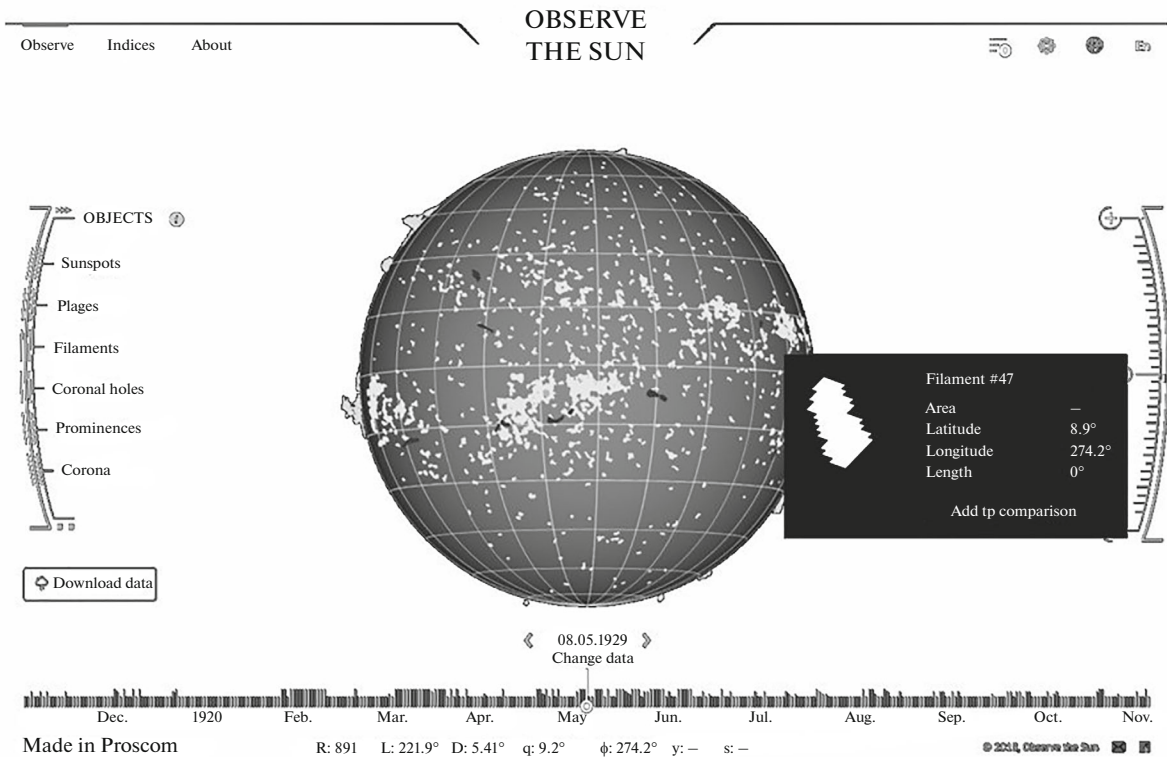


Fig. 9. Example of composite solar activity map published on website www.observethesun.com. Map for May 8, 1929 shows plages and elements of chromospheric network (according to Ca II K line data); sunspots from digitized data of RGO photoheliograms; filaments from Kodaikanal data in H-alpha line; and prominences from digitized data of visual observations with spectrohelioscopes. Window with information on specific filament is shown.

solar activity, was developed for this purpose (Illarionov and Tlatov, 2018). The functionality specified during the site's development, as well as the flexibility of the technologies implemented, allow it to be used for visualization and access to the data on the whole range of solar observations. This includes the observations of boundaries and parameters of the active regions, solar corona observations, various series of solar activity indices, and real-time forecasts. Part of the data is already available on the site, namely, for 1910, 1918–1932, 1959, and 2010–2018. Figure 8 illustrates the main page of the www.observethesun.com website.

7. CONCLUSIONS

The long-term data series presented in this study allow us to comprehensively reconstruct solar activity over an extended period of time. This provides an opportunity to study separate manifestations of solar activity, for example, solar filaments, sunspots, or prominences, as well as reveal the connection between the phenomena occurring at various latitudes and altitudes of the solar atmosphere.

An important feature of the study is the open access publication of all results on the Internet. In our opinion, this is a necessary condition for verifying the methods and it also facilitates a wider involvement of the collected data series in the scientific studies of short-period and long-period variations of solar activity.

ACKNOWLEDGMENTS

The study is supported by the Russian Foundation for Basic Research, project no. 18-02-00098-a, and the Russian Scientific Foundation, project no. 15-12-20001.

REFERENCES

- Bertello, L., Pevtsov, A., Tlatov A., and Singh, J., Correlation between sunspot number and Ca II K emission index, *Sol. Phys.*, 2016, vol. 291, pp. 2967–2979.
- Illarionov, E. A. and Tlatov, A.G., Development of a solar activity atlas, *Izv. Krym. Astron. Obs.*, 2018 (in press).
- Makarov, V.I. and Sivaraman, K.R., Poleward migration of the magnetic neutral line and the reversal of the polar fields on the sun. II. Period 1904–1940, *Sol. Phys.*, 1983, vol. 85, pp. 227–233.
- Makarov, V.I. and Sivaraman, K.R., Evolution of latitude zonal structure of the large-scale magnetic field in solar cycles, *Sol. Phys.*, 1989, vol. 119, pp. 35–43.
- McIntosh, P.S., Inference of solar magnetic polarities from H-alpha observations, in *Solar Activity Observations and Predictions* (Progress in Astronautics and Aeronautics), MIT, 1972, vol. 30, pp. 65–92.
- Ortiz, A. and Rast, M., How good is the Ca II K as a proxy for the magnetic flux?, *Mem. Soc. Astron. Ital.*, 2005, vol. 76, pp. 1018–1021.
- Pevtsov, A.A., Virtanen, I., Mursula, K., Tlatov, A., and Bertello, L., Reconstructing solar magnetic fields from historical observations. I. Renormalized Ca K spectroheliograms and pseudo-magnetograms, *Astron. Astro-phys.*, 2016, vol. 585, id A40.
- Tlatov, A.G., Pevtsov, A.A., and Singh, J., A new method of calibration of photographic plates from three historic data sets, *Sol. Phys.*, 2009, vol. 255, pp. 239–251.
- Tlatov, A., Tavastsherna, K., and Vasil'eva, V., Coronal holes in solar cycles 21 to 23, *Sol. Phys.*, 2014, vol. 289, pp. 1349–1358.
- Tlatov, A.G., Kuzanyan, K.M., and Vasil'eva, V.V., Tilt angles of solar filaments over the period of 1919–2014, *Sol. Phys.*, 2016a, vol. 291, no. 4, pp. 1115–1127.
- Tlatov, A.G., Skorbezh, N.N., and Ershov, V.N., *Numerical processing of sunspot images using the digitised long-term archive of the RGO observatory*, *ASP Conf. Ser.*, 2016b, vol. 504, p. 237.
- Tlatova, K.A. and Nagnibeda, V.G., Prominence characteristics in 16th activity cycle, *Geomagn. Aeron. (Engl. Transl.)*, 2017, vol. 57, no. 7, pp. 829–834.
- Tlatova, K.A., Vasil'eva, V.V., and Pevtsov, A.A., Long-term variations in the sunspot magnetic fields and bipole properties from 1918 to 2014, *Geomagn. Aeron. (Engl. Transl.)*, 2015, vol. 55, no. 7, pp. 896–901.
- Vasil'eva, V.V., Reconstruction of synoptic maps of large-scale magnetic fields for 1880–1914, in *Trudy konf.: Novyi tsikl aktivnosti Solntsa: nablyudatel'nye i teoreticheskie aspekty* (Proceedings of the Conference New Cycle of Solar Activity: Observational and Theoretical Aspects), St. Petersburg, GAO RAN, 1998, pp. 213–216.

Translated by M. Chubarova